Article

Re Variation Triggered from the Paleo-Pacific Plate Evolution: Constrains from Mo Polymetallic Deposits in Zhejiang Province, South China Mo Province

Xiangcai Li [1], Yongbin Wang [2,3,*], Xuance Wang [2,3], Jiaqi Cai [2], Yunkang Guo [2] and Song Lin [2]

[1] Faculty of Land Resources Engineering, Kunming University of Science and Technology, Kunming 650093, China
[2] Yunnan Key Laboratory of Earth System Science, Yunnan University, Kunming 650500, China
[3] Key Laboratory of Critical Minerals Metallogeny in Universities of Yunnan Province, Yunnan University, Kunming 650500, China
* Correspondence: wangyongbin0808@ynu.edu.cn

Abstract: Although highly dispersed, critical Re metal has attracted lots of attention from geoscientists, the controlling factors of Re-content variation are not completely understood, especially with regards to the genetic relationship between Re-bearing Mo polymetallic deposits and plate subduction evolution. It is well documented that the South China Mo Province, in Zhejiang Province, is characterized by multi-stage Mo polymetallic mineralization associated with Paleo-Pacific plate subduction. The Xianlin Mo(Cu)–Fe deposit occurs in Western Zhejiang as porphyry mineralization or skarn mineralization between the granodiorite and limestone. Zircon U–Pb analysis of the ore-forming granodiorite yields a Concordia age of 150.8 ± 1.1 Ma. Six molybdenite samples have relatively high Re contents (128.9~155.7 ppm) and deliver a weighted mean model age of 149.6 ± 1.3 Ma. These geochronological data suggest the Xianlin polymetallic mineralization was genetically related to the granodiorite in the Late Jurassic. Moreover, a new compilation of reliable Re contents and Re–Os isotope age data in Zhejiang Province indicates a decreasing trend in Re contents of molybdenite from the Jurassic Fe-/Cu-dominated Mo mineralization stage to the Cretaceous PbZn-enriched Mo mineralization stage in the South China Mo Province. Based on previously proposed models relating tectonic, magmatic, and hydrothermal processes, it is suggested that the Jurassic Re-enriched Mo mineralization, associated with I-type granitoids, formed in a compressive setting during the low-angle subduction of the Paleo-Pacific slab, whilst the Cretaceous Re-poorer Mo/Mo–Pb–Zn mineralization, related to both I- and A-type granitoids, formed in an extensional back-arc setting triggered by the rollback of the Paleo-Pacific slab.

Keywords: Zircon U–Pb; Re–Os isochron age; Xianlin; South China Mo Province

1. Introduction

Because of the extraordinary physicochemical properties of rhenium (Re), Re is broadly used in the high-temperature resistant superalloy, petroleum refining, and electronics industries. Hence, it has been listed as a critical metal by many countries, including the USA and China [1]. However, Re is one of the most particularly dispersed elements in the Earth's crust (<1 ppb, [2]) and, therefore, data on Re-bearing minerals are notably scarce [3,4]. Re is commonly generated commercially as a by-product of molybdenum of Mo polymetallic deposits, because the Re contents of molybdenite can be as excessive as thousands ppm [5]. However, Re contents of specific Mo polymetallic deposits are rather variable, consisting of Mo, Mo–Cu, Mo–Fe, Mo–W, Mo–PbZn, and Mo–Au [6,7], which may be allotted to precise geodynamic settings caused by means of plate subduction [8]. Therefore, the question concerning what type of porphyry deposit and tectonic setting is associated with the evolution of plate subduction and that has extra Re contents, calls for further studies.

Southeast China is characterized by the widespread occurrence of Mesozoic granitoids and mineralization, e.g., W, Sn, Cu, Pb, Zn, U, Nb, Ta, and Au [9]. In particular, recently discovered Mo deposits in this district have attracted more and more research, resulted in the defining of the South China Mo Province (SCMP [10]). Zhejiang Province, situated in the northeastern part of the SCMP (Figure 1a), is well endowed with granites and associated Mo polymetallic deposits, either inland or coastal [11–13]. Most research focused on Cretaceous Mo deposits, with limited studies on the Jurassic Mo mineralization. As a result, the Re contents of Cretaceous Mo or Mo–PbZn deposits are low, so whether or not high Re contents of the Jurassic Mo polymetallic deposits exist is still in its infancy. A series of Late Jurassic Mo polymetallic mineralization exists in the SCMP, i.e., the Dexing porphyry Cu–Mo deposit [14] and the Tongcun porphyry Cu–Mo deposit [11]. Therefore, comparing Jurassic and Cretaceous Mo deposits will help us to understand the regional Re-enriched mineralization regularity.

The Xianlin porphyry-skarn Mo(Cu)–Fe deposit, located in Zhejiang Province, could be an excellent case to improve our understanding of the Jurassic Re-enriched Mo mineralization and regularity in the SCMP. In the present study, we present zircon U–Pb ages for the ore-related granodiorite, and molybdenite Re–Os age for the Mo mineralization, to discuss the genetic relationships between mineralization and magmatism. The contents of Re have then been investigated in the molybdenites from the Xianlin porphyry-skarn Mo(Cu)-Fe deposit. Additionally, the spatial-temporal distribution of Re-bearing Mo mineralization will be documented. Furthermore, based on the regional tectonic-magmatic and hydrothermal activities in the Late Mesozoic, this study aims to highlight the priority tectonic setting for Re-enriched Mo mineralization in the SCMP.

2. Regional Geology

The South China Mo Province (SCMP), situated in the southeastern part of the South China Block, was amalgamated during the Late Neoproterozoic alongside the Jiangshan–Shaoxing Fault (JSF) between the Yangtze Craton and the Cathaysia block (Figure 1b, [15]). The complicated tectonic activities occurred in the SCMP from the Neoproterozoic to Mesozoic [16]. In particular, the northwestward subduction and rollback of the Paleo-Pacific plate under the South China Block took place in the Late Mesozoic [17,18], which resulted in widespread granite magmatism and intensive W–Sn–Cu–Au–Mo–Pb–Zn–Ag mineralization [9,12,19,20].

Zhejiang is located in the northeastern part of the SCMP (Figure 1b). The major tectonic units in Zhejiang are the Yangtze Craton in the northwest and the Cathaysia Block in the southeast (Figure 1b). The Yangtze Craton outcrops through the folded Proterozoic greenschist-facies basement and Paleozoic marine-facies sedimentary cover the area [21,22]. The Cathaysia Block can be subdivided into the Chencai–Suichang Uplift Belt and the Wenzhou–Linhai Depression Belt. The lithologies are composed of Proterozoic amphibolite-to granulite-facies metamorphic basement and overlying Mesozoic intermediate-acid volcanic rocks [23].

Late Mesozoic mineralization is significant in the Yangtze Craton in Northwestern Zhejiang and the Cathaysia Block in the Southeastern Zhejiang. Three episodes of Mo polymetallic mineralization in SCMP have been identified. Furthermore, they exhibit progressively younger ages towards the coast [9,18,24]. Stage 1, basically positioned in the Yangtze Block, consists of porphyry-skarn Cu–Mo and Fe–Mo mineralization related to I-type monzogranite and granodiorite at 170–145 Ma [11]. Stage 2, distributed alongside the JSF, is characterized by porphyry Mo and vein-type Pb–Zn–Ag mineralization related to I- and A-type granitoids at 145–125 Ma [25]. Stage 3, mainly in the Cathaysia Block, consists of granite-related porphyry Mo mineralization and epithermal Pb–Zn/Au–Ag mineralization at 125–90 Ma [12,19].
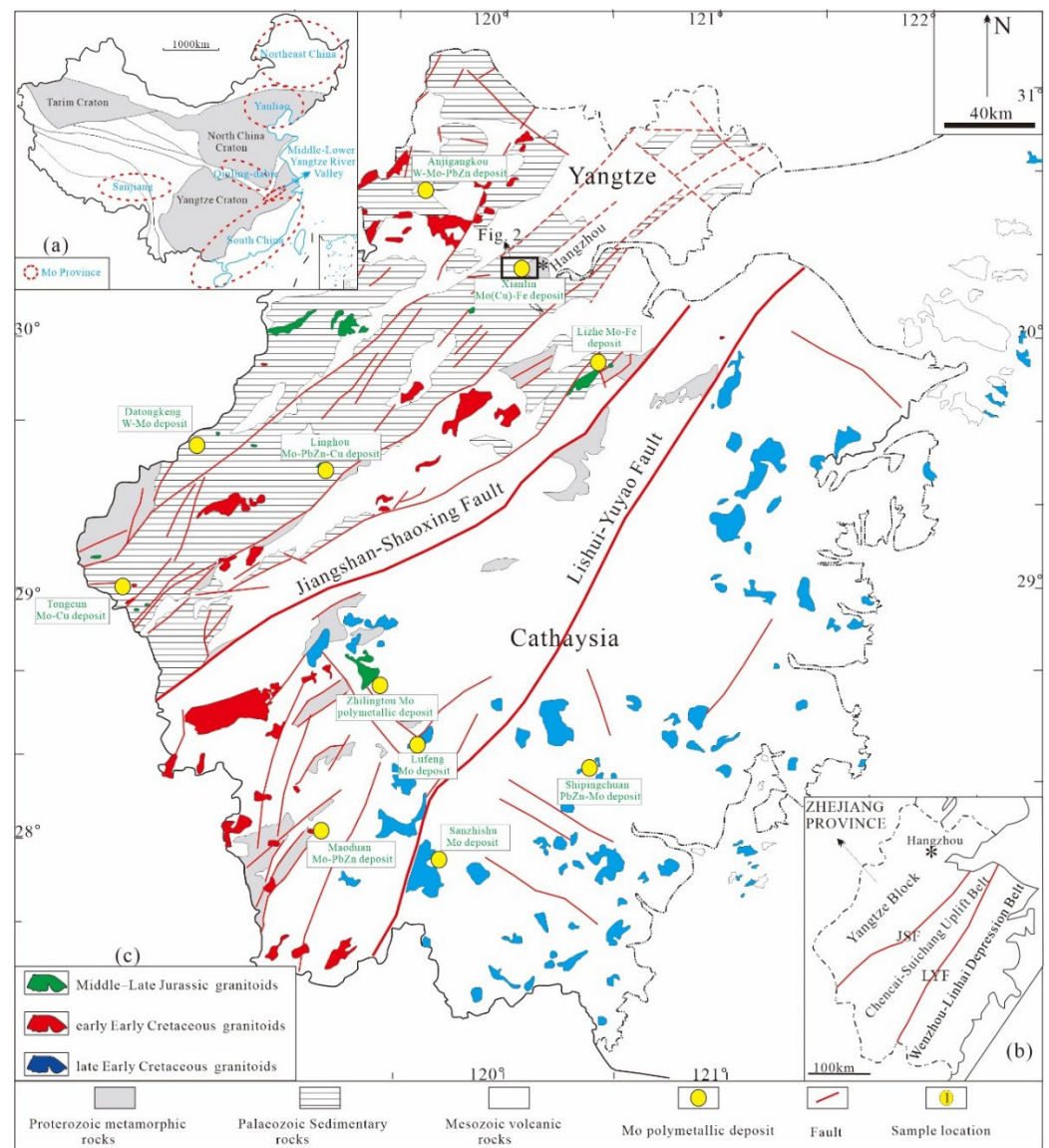
Figure 1. (**a**) distribution map of Mo metallogenic province in China [10]; (**b**) regional tectonic map of Zhejiang Province [26]; (**c**) simplified geological map of Zhejiang Province, showing the distribution of Mo polymetallic deposits [19,24].

3. Deposit Geology

The Xianlin Mo(Cu)–Fe deposit occurs in the northwestern part of Zhejiang Province, SCMP. The sedimentary lithologies cropping out in the mining area are Cambrian limestone and Quaternary. A set of NNE striking faults exist in the mining area (Figure 2). The faults have a total strike length of 1–2 km and dip to the southeast at the angles of 44–70°. The intrusive rocks, consisting of granodiorite and granite porphyry, are present in the deposit (Figure 3). The granodiorite in the ore field outcrops in an area of approximately 0.3 km², 1.1 km in length and 0.3 km in width, while the granite porphyry occurs as stock with 60 m in length and 0.7–3 m in width. Based on the crosscutting relationship, they are inferred to be the pre-mineralization and post-mineralization intrusions, respectively.
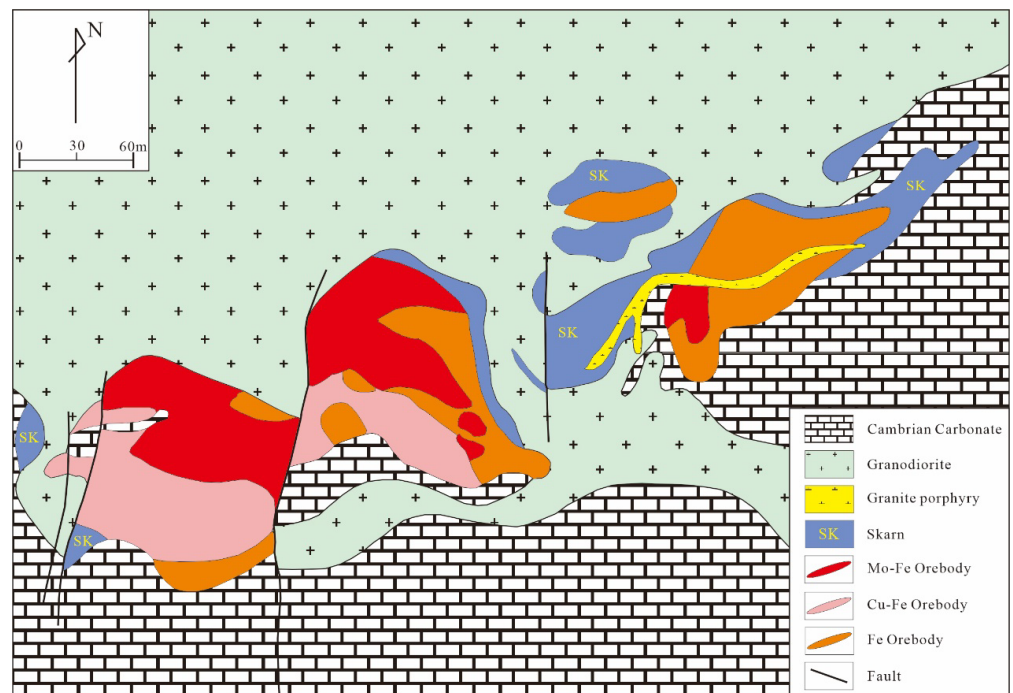
Figure 2. The geological map of the Xianlin Mo(Cu)-Fe deposit [26].
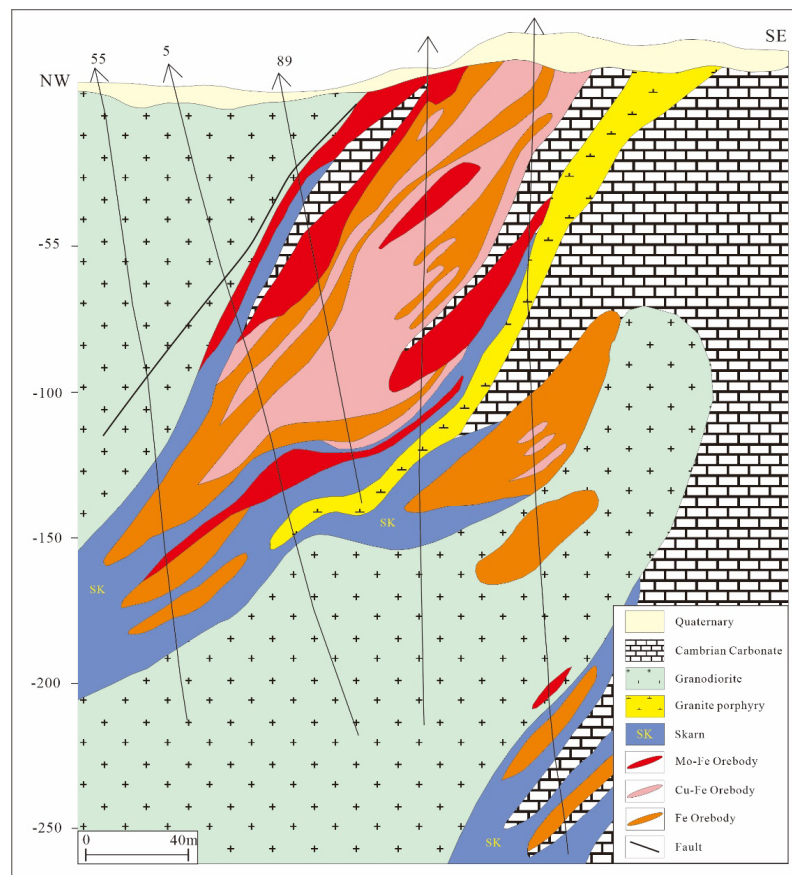

Figure 3. The geological cross-section of the exploration line of the Xianlin Mo(Cu)-Fe deposit [26].

The orebodies are characterized by porphyry- and skarn-type mineralization. The porphyry-type mineralization occurs as dissemination and stockwork in the granodiorite

(Figure 4a,b). The skarn-type mineralization is located at the contact between the granodiorite and limestone. The latter is more economically interesting than the former in the metal resources [26].
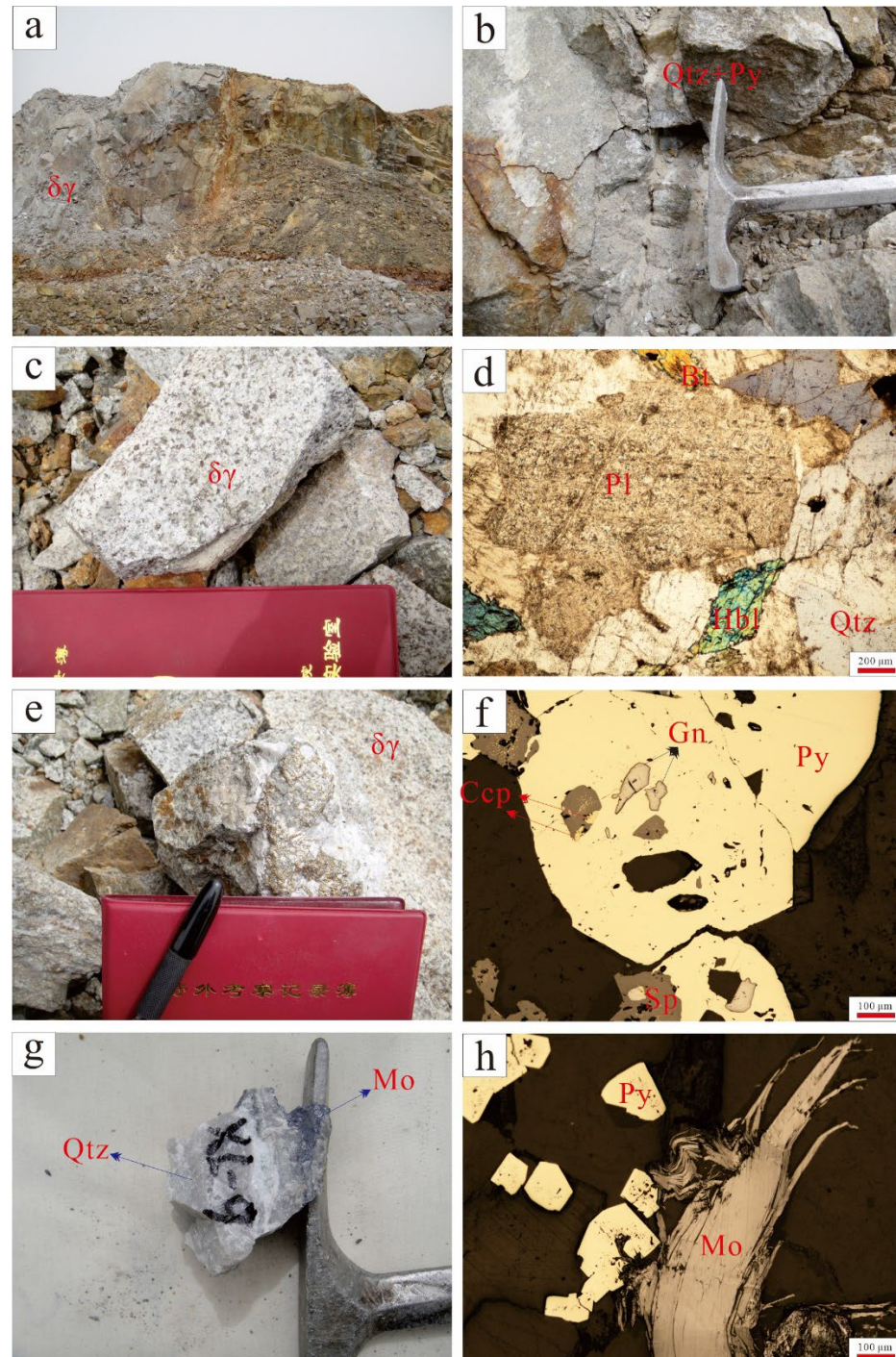
Figure 4. Macro- and micro-photographs of Mo mineralization within the granodiorite from Xianlin Mo(Cu)-Fe deposit: (**a**) open pit; (**b**) the quartz + pyrite + minor molybdenite vein; (**c**) mineralized granodiorite; (**d**) photomicrograph of mineralized granodiorite in the cross-polarized light; (**e**) granodiorite with disseminated pyrite; (**f**) microphotograph of ore, showing early pyrite partially replaced by late-stage galena, sphalerite, and chalcopyrite; (**g**) fragment of quartz-molybdenite vein; (**h**) pyrite and molydenite. δγ–Granodiorite; Pl–Plagioclase; Bt–Biotite; Hbl–Hornblende; Qtz–Quartz; Mo–Molybdenite; Py–Pyrite; Gn–Galena; Sp–Sphalerite; Ccp–Chalcopyrite.

The orebodies have been identified in two areas, consisting of the East Mining Area and the West Mining Area. One main orebody and some blind orebodies have been recognized in the East Mining Area. The largest orebody is approximately 144 m in length and extends to 177 m beneath the surface, with a maximum thickness of 70 m. The average grade of this lenticular orebody is 39.68% TFe. Moreover, the Cu-bearing and Mo-bearing orebodies are spread in the Fe orebodies. The Cu-bearing orebodies are approximately 97 m and 11 m in maximum thickness and 121 m in most vertical depth, with an average grade of 0.35%. The Mo-bearing orebodies are tiny and dispersed. They are approximately 22–50 m and 2–3 m in thickness, with 0.037–0.224% Mo. One main orebody and three blind orebodies were identified in the West Mining Area. The largest orebody is approximately 273 m in length, 250 m in depth, and has a maximum thickness of 75 m. The average grade of this orebody is 35.96% TFe and 0.0–0.229% Mo. Moreover, there are eight Cu-bearing and Mo-bearing orebodies, respectively. The grade of the most important Cu-bearing orebody is 0.25–0.46%. The grade of the main Mo orebody is 0.066–0.229%.

Hydrothermal alteration took place essentially with the granodiorite emplacement. Skarnization, silicification, sericitization, and carbonatization, are the dominant alteration types. The ore minerals are magnetite, pyrite, molybdenite, chalcopyrite, sphalerite, and galena (Figure 4e–h). The gangue minerals encompass quartz, diopside, garnet, and calcite.

4. Sample Description and Analytical Methods

4.1. Sample Description

The granodiorite (Xianlin–1) was sampled for the SIMS zircon U–Pb dating. The granodiorite shows an inequigranular texture (Figure 4c,d). It is composed of plagioclase (35–40 vol.%), quartz (20–30 vol.%), K-feldspar (20–30 vol.%), and biotite (<5 vol.%). The accessory minerals encompass magnetite, zircon, and apatite.

Six molybdenite samples have been obtained from quartz-molybdenite veinlets (XL–2, XL–3, XL–4, XL–6, XL–8, XL–11). Fresh samples have been handpicked to >99% in purity using the binocular microscope, then the molybdenite separates were crushed for analysis.

4.2. SIMS U–Pb Analysis

The zircon grains for the U–Pb isotope analysis, together with the zircon standards, including Plesovice and Qinghu, were mounted and polished for secondary ion mass spectrometry (SIMS) analysis. Th, U, and Pb isotopic ratios had been performed by the Cameca IMS-1280 SIMS at the Institute of Geology and Geophysics, Chinese Academy of Sciences, China. Analytical procedures are similar to those described by Li et al. (2009b) [27]. The measured compositions were corrected for common Pb using non-radiogenic ^{204}Pb. Data reduction was carried out using the software of the Isoplot 3.0.

4.3. ICP–MS Re–Os Analysis

Re–Os isotope analysis was carried out at the National Research Center of Geoanalysis, Chinese Academy of Geological Sciences, Beijing. The analytical procedures follow Du et al. (1994, 2004) [28,29]. The analyzed blanks were Re < 0.041 ng and ^{187}Os < 0.0002 ng. The Re–Os isochron was calculated and plotted by Isoplot 3.0. Re–Os model ages were calculated following the equation t = [ln(1 + ^{187}Os/^{187}Re)]/λ, where λ is 1.666 × 10^{-11} a^{-1}, which denotes the decay constant of ^{187}Re.

5. Results

5.1. Zircon U–Pb Dating

The zircons of the granodiorite (XL–1) from the Xianlin Mo(Cu)–Fe deposit are prismatic and euhedral, ranging from 120 to 300 μm and length-to-width ratios of 3:1 to 1:1. The zircon crystals exhibit well-developed oscillatory zoning (Figure 5a). All grains have higher Th/U ratios than metamorphic zircon (<0.1). The zircons are viewed as being of magmatic origin [30].
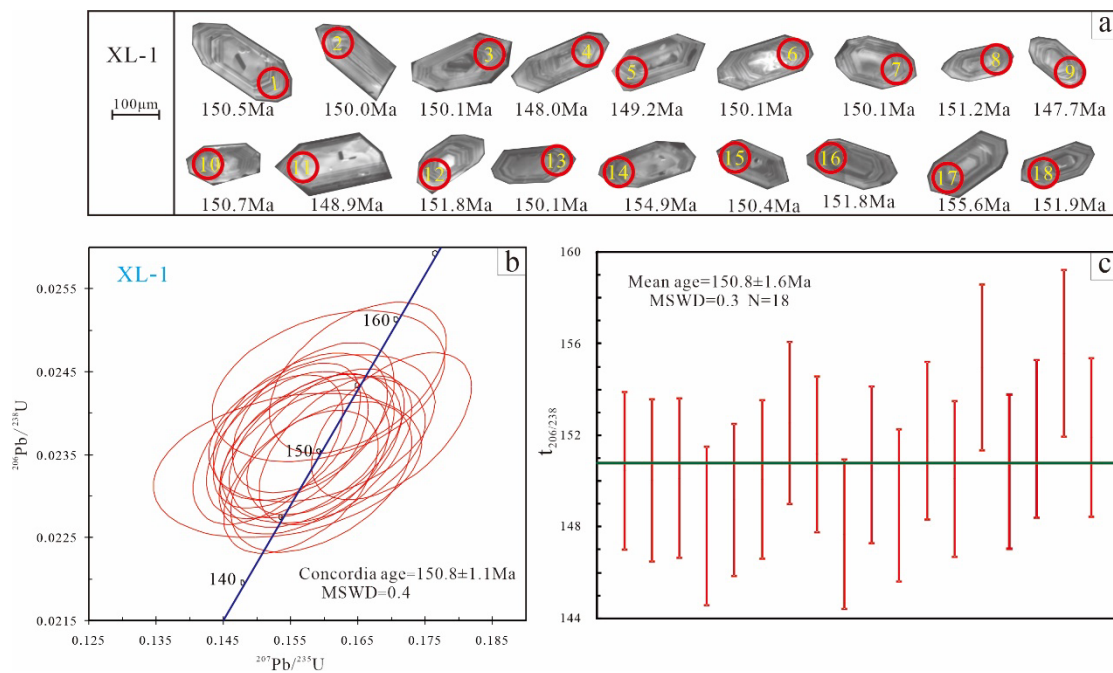
Figure 5. The cathodoluminescence (CL) image (**a**), SIMS U–Pb concordia diagram (**b**), and mean age diagram (**c**) of the zircon from the granodiorite in Xianlin Mo(Cu)-Fe deposit.

Eighteen analyses of the zircons from the sample XL–1 have been obtained. The results of U–Pb age are listed in Table 1. Th and U concentrations are relatively constant: Th = 39–140 μg/g, U = 109–318 μg/g with Th/U = 0.23–0.64. These analyses are concordant in $^{207}Pb/^{235}Pb$ and $^{206}Pb/^{238}U$ within analytical errors (Figure 5). They yield the Concordia age of 150.8 ± 1.1 Ma, consistent with the weighted mean $^{206}Pb/^{238}U$ age of 150.8 ± 1.6 Ma (MSWD = 0.3), which indicates the crystallization age of the pluton.

Table 1. SIMS U–Pb Zircon data of the granodiorite from the Xianlin Mo(Cu)-Fe deposit.

Sample	Th/ppm	U/ppm	Th/U	$f^{206}Pb$ (%)	Isotopic Ratios								Age (Ma)					
					$^{207}Pb/^{206}Pb$	±σ (%)	$^{207}Pb/^{235}U$	±σ (%)	$^{206}Pb/^{238}U$	±σ (%)			$t_{207/206}$	±σ	$t_{207/235}$	±σ	$t_{206/238}$	±σ
XL-1-1	119	238	0.5	0.00	0.04745	2.78	0.15450	3.17	0.0236	1.54			72.1	64.7	145.9	4.3	150.5	2.3
XL-1-2	99	235	0.4	0.20	0.04866	3.10	0.15798	3.48	0.0235	1.60			131.5	71.2	148.9	4.8	150.0	2.4
XL-1-3	91	237	0.4	0.00	0.04669	2.56	0.15166	3.00	0.0236	1.56			33.1	60.2	143.4	4.0	150.1	2.3
XL-1-4	102	233	0.4	0.15	0.04982	3.06	0.15956	3.45	0.0232	1.59			186.4	69.8	150.3	4.8	148.0	2.3
XL-1-5	126	318	0.4	0.19	0.04864	2.91	0.15700	3.28	0.0234	1.51			130.5	67.1	148.1	4.5	149.2	2.2
XL-1-6	111	253	0.4	0.00	0.04978	2.41	0.16165	2.87	0.0235	1.56			184.9	55.2	152.1	4.1	150.1	2.3
XL-1-7	80	208	0.4	0.17	0.04797	2.70	0.15837	3.11	0.0239	1.55			97.8	62.7	149.3	4.3	152.5	2.3
XL-1-8	139	254	0.5	0.35	0.04720	2.48	0.15443	2.90	0.0237	1.51			59.5	58.1	145.8	4.0	151.2	2.3
XL-1-9	140	256	0.5	0.05	0.04899	2.58	0.15652	3.00	0.0232	1.52			147.2	59.5	147.7	4.1	147.7	2.2
XL-1-10	90	224	0.4	0.32	0.04912	2.55	0.16017	2.97	0.0237	1.52			153.3	58.7	150.9	4.2	150.7	2.3
XL-1-11	46	109	0.4	0.34	0.04795	5.04	0.15452	5.27	0.0234	1.52			96.9	115.3	145.9	7.2	148.9	2.2
XL-1-12	133	209	0.6	0.17	0.04861	4.02	0.15964	4.30	0.0238	1.52			128.9	92.0	150.4	6.0	151.8	2.3
XL-1-13	39	170	0.2	0.00	0.04923	3.55	0.15989	3.87	0.0236	1.53			158.7	81.1	150.6	5.4	150.1	2.3
XL-1-14	66	146	0.4	0.00	0.04788	4.12	0.16061	4.40	0.0243	1.53			93.5	94.8	151.2	6.2	154.9	2.3
XL-1-15	131	282	0.5	0.08	0.04858	2.79	0.15811	3.17	0.0236	1.51			127.4	64.3	149.0	4.4	150.4	2.2
XL-1-16	130	251	0.5	0.20	0.04760	3.03	0.15644	3.39	0.0238	1.52			79.6	70.4	147.6	4.7	151.8	2.3
XL-1-17	65	183	0.4	0.00	0.04897	2.88	0.16493	3.26	0.0244	1.52			146.3	66.2	155.0	4.7	155.6	2.3
XL-1-18	116	240	0.5	0.00	0.05171	2.42	0.17000	2.85	0.0238	1.52			272.6	54.4	159.4	4.2	151.9	2.3

5.2. Molybdenite Re–Os Dating

The Re–Os data for the molybdenite from the Xianlin Mo(Cu)–Fe deposits are listed in Table 2. It must be noted that the elemental Re contents vary from 128.9 to 155.7 μg/g, which are relatively high values in the context of the deposits of the SCMP. The samples define an isochron age of 146 ± 12 Ma (MSWD = 0.4). The Re–Os model ages of the six molybdenite samples show a narrow range between 149.1 and 150.3 Ma with a weighted mean age of 149.6 ± 1.3 Ma (Figure 6b). The weighted mean age is consistent with the

isochron age within the error, which can be explained as the age of Mo mineralization in the Xianlin Mo(Cu)–Fe deposit.

Table 2. Re–Os isotope data for molybdenite samples from the porphyry Mo orebodies from the Xianlin deposit.

Sample	Brief Sample Description	Weight (g)	Re (µg/g)		^{187}Re (µg/g)		^{187}Os (ng/g)		Model Age (Ma)	
			Measured	2σ	Measured	2σ	Measured	2σ	Measured	2σ
XL-2	Molybdenite-quartz vein	0.01018	128.90	1.00	81.00	0.60	202.99	1.75	150.2	2.1
XL-3	Molybdenite-quartz vein	0.01048	147.00	1.40	92.40	0.88	230.91	1.90	149.8	2.2
XL-4	Molybdenite-quartz vein	0.01016	141.90	1.10	89.18	0.68	221.98	1.75	149.2	2.0
XL-6	Molybdenite-quartz vein	0.01046	155.70	1.20	97.85	0.77	243.80	2.40	149.4	2.2
XL-8	Molybdenite-quartz vein	0.01038	142.50	1.20	89.56	0.73	222.71	1.77	149.1	2.1
XL-11	Molybdenite-quartz vein	0.01046	144.80	1.30	90.99	0.84	228.13	1.87	150.3	2.2

Notes: All the data are calculated using the decay constant λ (^{187}Re) = 1.666 $\times$ 10^{-11}/a [31].
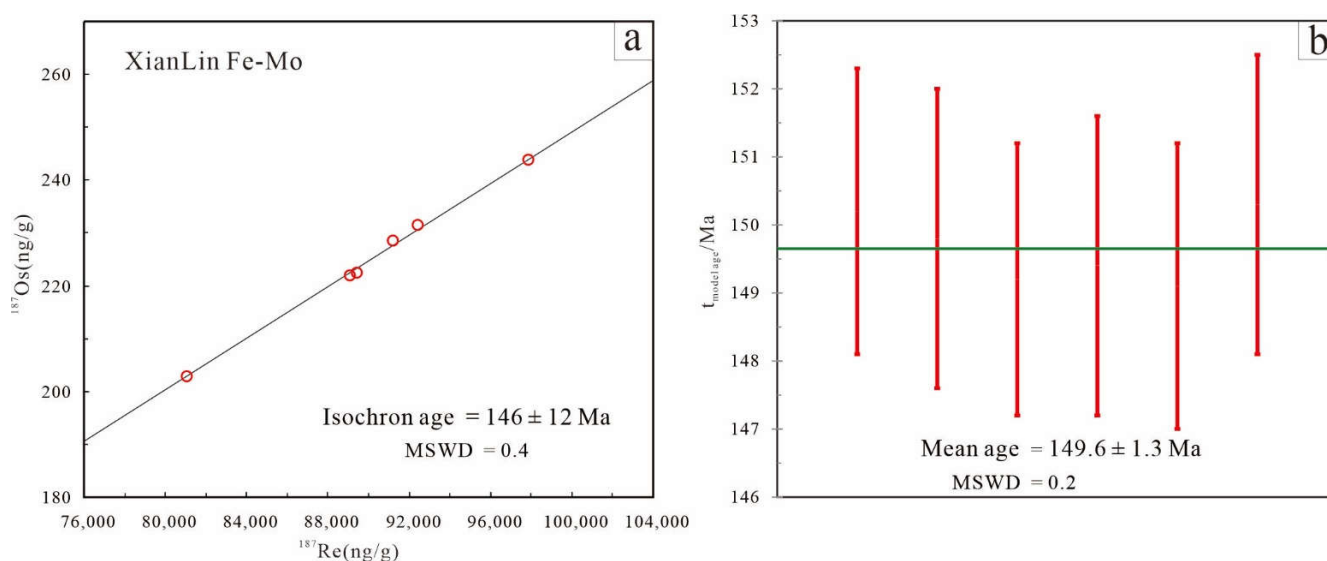

Figure 6. Re–Os isochron diagram (**a**) and mean age diagram (**b**) for molybdenite samples from the Xianlin Mo(Cu)-Fe deposit.

6. Discussion

6.1. The Jurassic Re-Enriched Mo Mineralization in the SCMP

The Mo(Cu)-Fe orebodies are characterized by porphyry- and skarn-type mineralization and more occur at the contact between the granodiorite and limestone. Skarnization, silicification, sericitization, and carbonatization, are mainly developed around the granodiorite. In particular, the Mo mineralization occurs as disseminated in the granodiorite or lenticular within the Fe orebodies. These features indicate that the Mo(Cu)-Fe mineralization was temporally and spatially associated with the granodiorite. Moreover, the granodiorite has SiO$_2$ contents of 60.46–66.96 wt.%, and it has high alkali concentrations (K$_2$O + Na$_2$O = 7.07–7.56 wt.%; A/CNK = 0.85–0.96), moderate Al (Al$_2$O$_3$ = 14.62–17.43 wt.%), Ca and Fe contents, and low Mg, Ti and P contents [32]. Combed with the presence of the hornblende in the intrusion (Figure 4d), this indicates that the granodiorite belongs to I-type granite. In this study, the U–Pb isotopic age shows that the crystallization age of the granodiorite is 150.8 ± 1.1 Ma. Moreover, the Re–Os isochronal dating of the six samples yielded a weighted mean age of 149.6 ± 1.3 Ma, representing the ore-forming age in the Xianlin Mo(Cu)-Fe deposit. The agreement in the ages between granodiorite intrusion and Mo mineralization suggests that Xianlin polymetallic mineralization was genetically related to the formation of granodiorite in the Late Jurassic.

Meanwhile, the total Re contents of the molybdenites from the Xianlin Mo(Cu)–Fe deposit range from 128.9 to 155.7 µg/g. Moreover, Zeng et al. (2012) [11] reported that the Re

contents of the Late Jurassic Tongcun Mo–Cu deposit in the Western Zhejiang Province vary from 36.6 to 121.7 µg/g. Wang et al. (2013) [33] reported that the Re-Os isochron age of the molybdenite from the LiZhu Fe-Mo deposit in the Western Zhejiang Province is 149.3 Ma. Hu et al. (2016) [34] showed that the Re–Os isochron age of the molybdenite from Datongkeng W-Mo deposit in the Western Zhejiang Province is 146.5 ± 0.8 Ma with the Re contents of 9.7~116.7 µg/g. Tang et al. (2017) [35] obtained a Re–Os age of 162.2 ± 1.4 Ma for the Linghou Mo–PbZn–Cu deposit in the Western Zhejiang Province with the Re contents of 195.4~226.3 µg/g. In addition, a series of Re-enriched porphyry-skarn deposits in the Jurassic have been discovered in the northwestern part of the SCMP, including Tongchang orefield (Re: 416.9~1571 µg/g, 171.1 Ma), Fujiawu orefield (Re: 180.1~652.5 µg/g, 171.1 Ma), and Zhushahong orefield (Re: 100.1~933.7 µg/g, 170 Ma) in the Dexing porphyry Cu–Mo deposit [14]. Compared to W–Mo deposits, the Re-enriched Mo deposits in this stage are characteristic by Cu-dominated or Fe-dominated polymetallic systems related to granite porphyry and granodiorite in the Middle-Late Jurassic (170–145Ma). These data indicate an extensive magmatic-hydrothermal Re-enriched Mo mineralization event in the SCMP.

6.2. The Spatial-Temporal Distribution of Re-Bearing Mo Mineralization

Based on the Re contents of the single Mo polymetallic deposit, these factors could be related to the petrogenesis of the host rock and ore-genesis of the molybdenite [6,36]. However, the lack of observable correlation between molybdenite Re concentration and geologic features of regional Mo polymetallic deposits hamper understanding of the Re-bearing mineralization regularity. Zhejiang Province in Southeast China is an essential region of Late Mesozoic Mo polymetallic mineralization in the SCMP. Based on the new accumulated reliable data (Table 3), three stages of the Mo polymetallic deposits have been recognized (Figure 7): Stage I (170–145 Ma), Stage II (145–125 Ma), and Stage III (125–90 Ma).

Table 3. The characteristics of Mo polymetallic deposits in the Zhejiang province, South China Mo Province.

Deposit	Metal Association	Deposit Type	Ore Minerals	Gangue Minerals	Ore-Forming Intrusion	Mineralization Age	Re (µg/g)	References
Tongcun	Mo-Cu	Porphyry-skarn	Mo, Ccp, Py	Qtz, Ser, Cal, Grt, Ep, Chl	Granite porphyry (169.7Ma)	163.9Ma	36.6–121.7	[10]
Linghou	Mo-PbZn-Cu	Porphyry-skarn	Py, Ccp, Mo, Sp, Gn, Po	Qtz, Chl, Fl, Kao	Granodiorite porphyry (160.6Ma)	162.2Ma	195.4–226.3	[35]
Xianlin	Mo(Cu)-Fe	Porphyry-skarn	Mag, Py, Mo	Grt, Qtz, Ser, Cal	Granodiorite (147.2Ma)	149.6Ma	128.9–155.7	This study
Lizhe	Mo-Fe	Porphyry-skarn	Mag, Py, Mo	Grt, Qtz, Ser, Cal	Granite (150.1Ma)	149.3Ma		[33]
Datongkeng	W-Mo	Porphyry-skarn	Py, Mo, Sch, Ccp, Mag, Sp, Gn	Qtz, Ser, Ch, Cal, Di,	Granite (148.3Ma)	146.5Ma	9.7–116.7	[34]
Anjigangkou	W-Mo-PbZn	Porphyry-skarn	Py, Mo, Sch, Sp, Gn	Grt, Qtz, Ser, Cal	Granodiorite (141.0Ma)	138.5Ma		[37]
Maoduan	Mo-PbZn	Porphyry	Py, Mo, Sp, Gn, Po	Qtz, Chl, Fl, Kao	Monzogranite (140Ma)	137.7Ma	3.1–7.9	[25]
Zhilingtou	Mo-PbZn-AuAg	Porphyry	Py, Mo, Sp, Gn	Qtz, Ser, Fl, Cal, Chl	Granite porphyry (113.6Ma)	113Ma	14.5–58.6	[20]
Sanzhishu	Mo	Porphyry	Mo, Py	Qtz, Ser, Fl, Cal, Chl	Monzogranite (112.3Ma)	112Ma	15.7–25.7	[12]
Lufeng	Mo	Porphyry	Mo, Py	Kf, Qtz, Ser, Cal	Granite porphyry (108.4Ma)	108Ma	4–10.7	[19]
Shipingchuan	Mo-PbZn	Porphyry	Mo, Py	Qtz, Ser, Fl	Syenogranite (107.5Ma)	104.7Ma	1.3–45.6	[38]

Notes: All ore-forming intrusion ages were determinate by U–Pb dating. All mineralization ages were obtained by Re-Os dating. Mineral observations: Kf–K-feldspar; Ser–Sericite; Chl–Chlorite; Fl–Fluorite; Kao–Kaolinite; Toz–Topaz; Di–Diopside; Grt–Garnet; Cal–Calcite; Mo–Molybdenite; Py–Pyrite; Sp–Sphlerite; Gn–Galena; Ccp–chalcopyrite; Po–Pyrrhotite; Wf–wolframite.
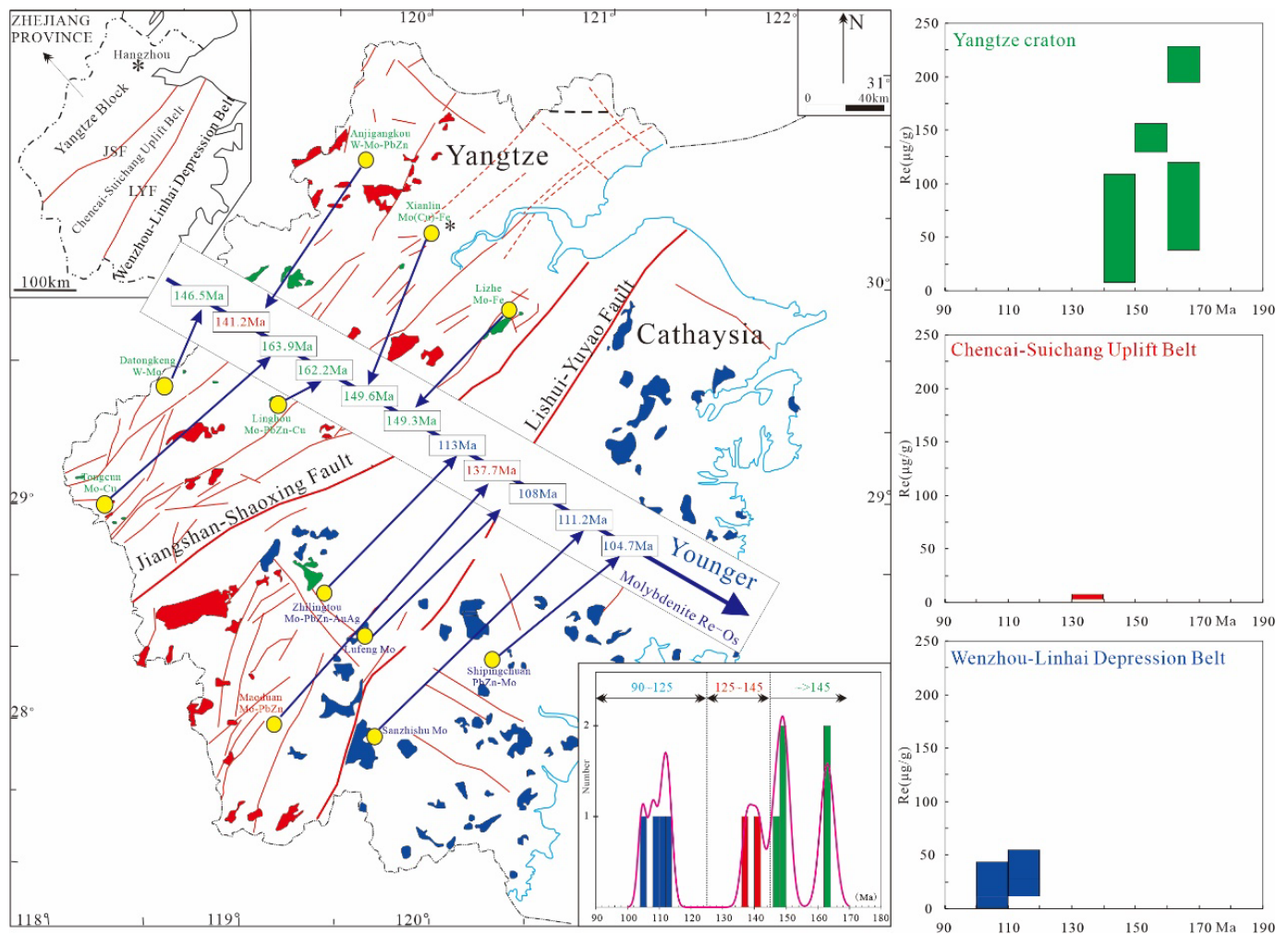
Figure 7. The distribution map and cumulative probability diagram of isotopic ages for the Mo polymetallic deposits in Zhejiang Province, showing the variation of Re content in molybdenite from the three-stage Mo polymetallic deposits.

Stage I (170–145 Ma): The Mo polymetallic systems include porphyry Mo–Cu and Mo–Fe deposits, such as Linghou Mo–PbZn–Cu deposit (Re: 195.4–226.3 μg/g), Tongcun Mo–Cu deposit (Re: 36.6–121.7 μg/g), Xianlin Mo–Fe deposit (Re: 128.9–155.7 μg/g), and Datongkeng W–Cu–Mo deposit (Re: 9.7–116.7 μg/g), in the Yangtze Mo metallogenic belt.

Stage II (145–125 Ma): Li et al. (2012) [25] confirmed that the molybdenite Re–Os isochron age is 137.7 ± 2.7 Ma from the Moduan Mo–PbZn deposit with the Re contents of 3.1–7.9 μg/g. Moreover, Tang et al. (2013) [37] stated that the Re–Os isochron age of the molybdenite is 141.2 ± 1.1 Ma from the Anjigangkou W–Mo–PbZn deposit. Previous Re–Os dating of molybdenite has revealed some Mo mineralization events during 136–134 Ma in the SCMP. The Maoduan monzogranite samples are high in silica, potassium, and plot, in the high-K calc-alkaline series. The granites are metaluminous to weakly peraluminous.

Stage III (125–90 Ma): The presence of this stage of Mo polymetallic deposits was identified in Zhejiang Province, including the Zhilingtou Mo–PbZn–AuAg (113 ± 2.4 Ma; Re: 14.5–58.6 μg/g. [11,20]), Sanzhishu Mo deposit (111.2 ± 6.4 Ma; Re: 15.7–25.7 μg/g. [12]), the Lufeng Mo deposit (108 ± 1.8 Ma; Re: 4–10.7 μg/g. [19]), and Shipingchuan PbZn–Mo (104.7 ± 1 Ma; Re: 1.3–45.6 μg/g. [38]). A compilation of reliable data suggests that the Re contents of this stage of Mo mineralization are low (1.3–58.5 μg/g) in the SCMP.

6.3. Geodynamic Setting of the Re-Bearing Mo Mineralization

Although a series of factors have been proposed, which includes the nature of the ore-forming fluids and petrogenesis of the ore-forming rocks, the controlling factors of Re-content variant are not neatly explained [6,36]. Mineral deposits are heterogeneous, however, the physical process for their genesis is commonly related to the specific magmatism and the tectonic setting [39]. In particular, Chen et al. (2017) [8] emphasized that the spatial-temporal distribution pattern of Mo polymetallic systems can be a diagnostic signature of specific tectonic settings in conjunction with petrogenetic-tectonic evidence. Further assessment of these hypotheses would be required to address the Re concentration of different Mo polymetallic systems in different tectonic settings. Based on integrating previous tectonic-magmatic and hydrothermal activities in the Late Mesozoic, this study attempts to discuss the coupling relationship between the tectonic setting triggered by the subduction evolution of the Paleo-Pacific Ocean plate and the Re-related Mo polymetallic deposits in Zhejiang Province, SCMP.

Stage I (170–145 Ma): Stage I high-Re Mo polymetallic deposits in the Yangtze Craton of Western Zhejiang encompass Linghou Mo–PbZn-Cu deposit, Tongcun Mo–Cu deposit, Xianlin Mo(Cu)–Fe deposit, Lizhe Mo–Fe deposit, and Datongkeng W–Cu–Mo deposit, which are genetically related to granodiorite and granite alongside a NE-striking in the Yangtze Craton. These intrusions are associated I-type granitoids with high SiO_2, Al_2O_3, and total alkali ($K_2O + Na_2O$) concentrations [34,35,40,41]. These granitoids are enriched in LREEs and Sr contents, depleted in HREEs and Yb contents, and exhibit slender negative Eu anomalies, indicating that the presence of residual garnet existed during magma genesis [24]. The Sr/Y–Y analyses show that the Jurassic magmatism was mostly adakitic (Figure 8), together with previous experimental studies of adakitic rocks [42], suggesting a thickened lower crust (>50 km) in the Middle-Late Jurassic [7,43]. Sr–Nd–Hf isotopic compositions point out that the granitoids may have crystallized from hybrid magmas of Mesoproterozoic crust-derived and depleted mantle-derived magmas [24]. The petrogenesis of these granitoids indicated that the Paleo-Pacific plate penetrated beneath the South China hinterland at a shallowly dipping angle, and generated an active continental margin setting in the Early Jurassic [44]. As subduction continued, the fluids liberated from the descending slab produced partial melting in the overlying mantle wedge. These metal-enriched melts migrated upwards, producing a range of granitic rocks and Mo polymetallic deposits (Figure 9a).
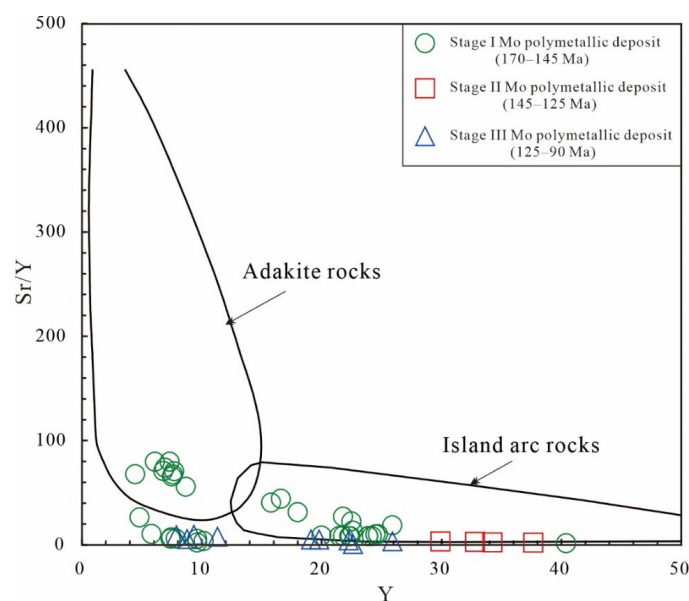

Figure 8. (Sr/Y) vs. Y diagram for the Mo-related Late Mesozoic granites in Zhejiang Province, SE China [45].
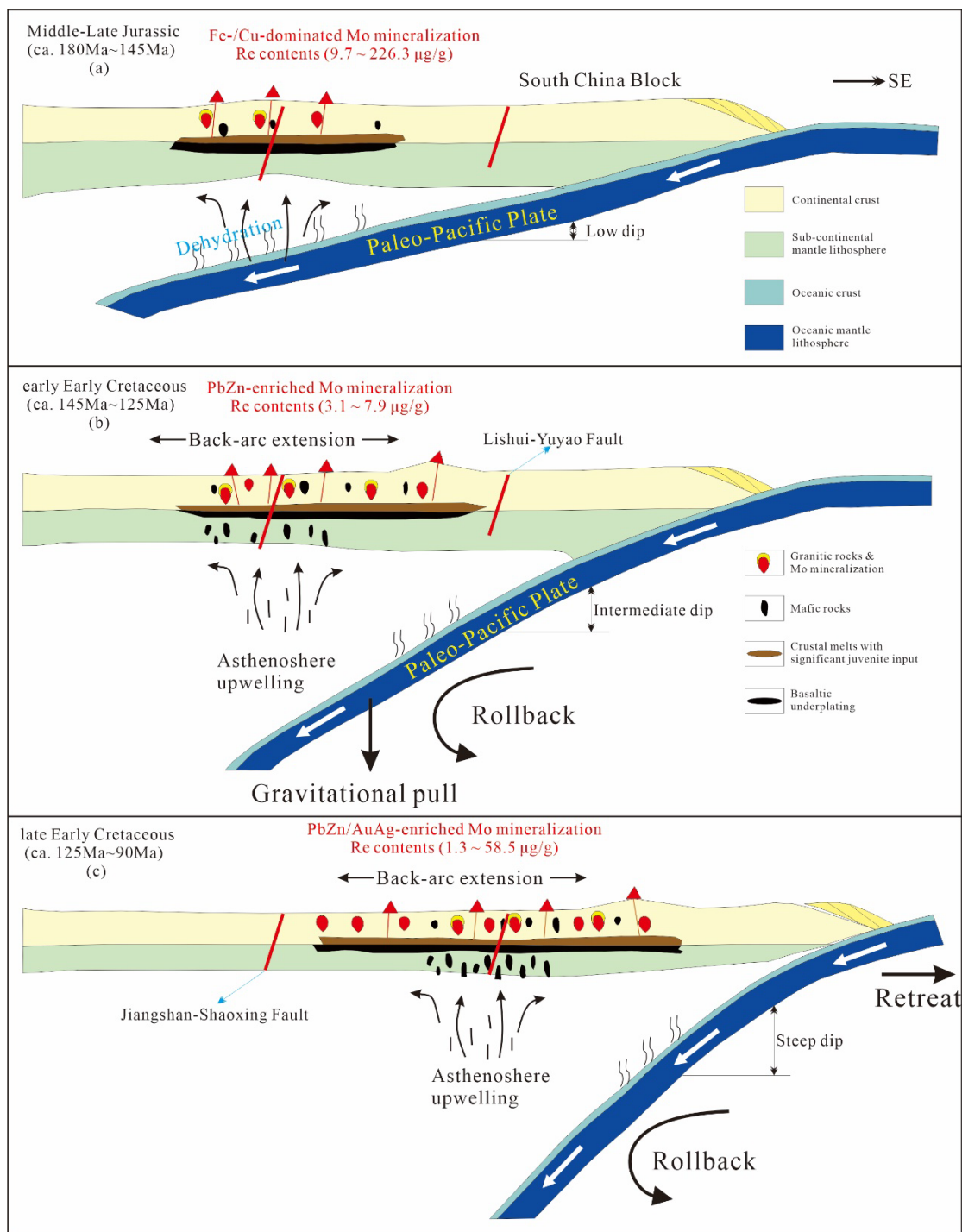
Figure 9. The tectono-magmatic-mineralization evolution model of the Paleo-Pacific plate subduction in Zhejiang Province in the SCMP during the Late Mesozoic. (**a**) the low-dipping-angle subduction of the Paleo-Pacific plate in the Stage I (170–145 Ma); (**b**) the rollback beginning of the Paleo-Pacific plate in the Stage II (145–125 Ma); (**c**) the progressive rollback and retreat of the Paleo-Pacific plate in the Stage III (125–90 Ma). Modified from Wang et al., 2018 [24].

Stage II (145–125 Ma): Stage II low-Re Mo polymetallic deposits, positioned basically inland, are genetically associated with highly fractionated I-type or high-K I-type monzogranites or granites, alongside the Jiang–Shao Fault Zone in Zhejiang Province [25]. The contemporary granitoids are characterized by high TFe_3O_4/MgO ratios, LILE enrichment, HFSE depletion, negative Eu anomalies, and depletions in Ba, Sr, P, Eu, and Ti [24].

These granitoids are characterized by low Sr/Y and La/Yb ratios and plot primarily in the field of island arcs, as seen in Figure 8. Combing the previous Sr–Nd–Hf isotopic compositions [24], we infer that these rocks were derived from the partial melting of the lower crust contaminated by enriched mantle at depths of <50 km [42]. Meanwhile, A-type granitoids in the northwestern part of Zhejiang Province in the Early Cretaceous (ca. 145–120 Ma) indicate that back-arc extension initiated as early as ~145 Ma [46,47]. Previous studies indicated that the beginning of the rollback of the Paleo-Pacific slab caused strong asthenosphere–lithosphere interaction for the formation of the I- and A-type granites. It could be most probably attributed to the elevated gravitational pull on the subduction slab from a low-angle to a medium-angle [24]. The rollback is supported by the youngling trend of magmatic and mineralization belts migrating from inland towards coastal (Figure 9b).

Stage III (125–90 Ma): Stage III Mo polymetallic deposits are distributed alongside the Lishui–Yuyao Fault Zone [48]. They belong to the High-F but low-Re Mo mineralization related to A-type or notably fractionated I-type granite [12,19,36]. The granites in this stage are comparable to those of the early stage but with more evidently negative Eu anomalies and higher LREEs contents, as well as more involvement of juvenile material as indicated by higher $\varepsilon_{Hf}(t)$ values of −11.6 to +4.5 and $\varepsilon_{Nd}(t)$ values of −10.82 to −0.7 [49,50]. These features indicate greater mantle involvement for this stage of magmatic-hydrothermal event in a stronger lithospheric extensional setting. These granitoids also belong to island arc rocks in the Sr/Y–Y diagrams but have lower Sr/Y and La/Yb ratios than the Stage II granitoids (Figure 8), indicating crustal thickness is much less than 50 km [51]. The regional extension migrated from the inland to the coastal area. This is probably attributed to progressive rollback and retreat of the Paleo-Pacific slab [52]. In this stage, the upwelling of the asthenosphere induced partial melting of mantle and crustal rocks, producing granitic magmas and extensive Mo mineralization (Figure 9c).

7. Conclusions

(1) Our zircon U–Pb (150.8 ± 1.1 Ma) and molybdenite Re–Os (149.6 ± 1.3 Ma) ages of the Xianlin porphyry-skarn Mo(Cu)–Fe deposit indicate that a significant magmatic event was associated with the Re-enriched Mo mineralization in the SCMP.

(2) This study indicates that a decreasing trend in Re content from the Jurassic Mo–Cu/Mo–Fe mineralization stage (170–145 Ma) to the Cretaceous Mo/Mo–PbZn mineralization stage (145–90 Ma) in the SCMP.

(3) The Paleo-Pacific plate played a crucial role in the Late Mesozoic tectonic-magmatic development of Zhejiang Province, SCMP, especially, influencing the spatial and temporal distribution of Re contents from different Mo polymetallic deposits. Jurassic Re-enriched Mo–Cu/Mo–Fe mineralization associated with I-type granitoids was formed in an active continental margin triggered by the low-angle subduction of the Paleo-Pacific slab. Cretaceous Re-low Mo/Mo–PbZn mineralization related to I- and A-type granitoids was formed in an extensional back-arc environment triggered by the rollback of the Paleo-Pacific slab.

given to Andao Du, Wenjun Qu, and Chao Li, from the Institute of Mineral Resources, Chinese Academy of Geology.

References

1. Mao, J.W.; Yang, Z.X.; Xie, G.Q.; Yuan, S.D.; Zhou, Z.H. Critical minerals: International trends and thinking. *Miner. Deposit.* **2019**, *38*, 689–698. (In Chinese with English Abstract).
2. Taylor, S.R.; MacLennan, S.M. *The Continental Crust: Its Composition and Evolution*; Blackwell Scientific Publications: Palo Alto, CA, USA, 1985.
3. Korzhinsky, M.A.; Tkachenko, S.I.; Shmulovich, K.I.; Taran, Y.A.; Steinberg, G.S. Discovery of a pure rhenium mineral at Kudriavy volcano. *Nature* **1994**, *369*, 51–52. [CrossRef]
4. Liao, R.Q.; Liu, H.; Li, C.Y.; Sun, W.D. Rhenium resource exploration prospects in China based on its geochemical properties. *Acta Petrol. Sin.* **2020**, *36*, 55–67. (In Chinese with English Abstract).
5. Huang, F.; Wang, D.H.; Wang, Y.; Jiang, B.; Li, C.; Zhao, H. Study on metallogenic regularity rhenium deposits in China and their prospecting direction. *Acta Geol. Sin.* **2019**, *93*, 1252–1269. (In Chinese with English Abstract).
6. Berzina, A.N.; Sotnikova, V.I.; Economou-Eliopoulosb, M.; Eliopoulos, D.G. Distribution of rhenium in molybdenite from porphyry Cu–Mo and Mo–Cu deposits of Russia (Siberia) and Mongolia. *Ore Geol. Rev.* **2005**, *26*, 91–113. [CrossRef]
7. Wang, J.B.; Zou, T.; Wang, Y.W.; Long, L.L.; Zhang, H.Q.; Liao, Z.; Xie, H.J. Deposit associations, metallogenesis and metallogenic lineage of molybdenum-polymetallic deposits in China. *Miner. Deposit.* **2014**, *33*, 447–470. (In Chinese with English Abstract).
8. Chen, Y.J.; Zhang, C.; Wang, P.; Pirajno, F.; Li, N. The Mo deposits of Northeast China: A powerful indicator of tectonic settings and associated evolutionary trends. *Ore Geol. Rev.* **2017**, *81*, 602–640. [CrossRef]
9. Mao, J.W.; Cheng, Y.B.; Chen, M.H.; Pirajno, F. Major types and time-space distribution of Mesozoic ore deposits in South China and their geodynamic settings. *Miner. Depos.* **2013**, *48*, 267–294.
10. Zeng, Q.D.; Liu, J.M.; Qin, K.Z.; Fan, H.R.; Chu, S.X.; Wang, Y.B.; Zhou, L.L. Types, characteristics, and time–space distribution of molybdenum deposits in China. *Int. Geol. Rev.* **2013**, *55*, 1311–1358. [CrossRef]
11. Zeng, Q.D.; Wang, Y.B.; Zhang, S.; Liu, J.M.; Qin, K.Z.; Yang, J.H.; Sun, W.D.; Qu, W.J. U–Pb and Re–Os geochronology of the Tongcun molybdenum deposit and Zhilintou gold-silver deposit in Zhejiang province, Southeast China, and its geological implications. *Resour. Geol.* **2012**, *63*, 99–109. [CrossRef]
12. Wang, Y.B.; Zeng, Q.D.; Liu, J.M.; Pirajno, F. Cretaceous magmatism and Mo mineralization in the South China Mo Province: U–Pb and Re–Os geochronology constraints from the Sanzhishu porphyry Mo deposit. *Ore Geol. Rev.* **2017**, *81*, 912–924. [CrossRef]
13. Zhong, J.; Chen, Y.J.; Pirajno, F. Geology, geochemistry and tectonic settings of the molybdenum deposits in South China: A review. *Ore Geol. Rev.* **2017**, *81*, 829–855. [CrossRef]
14. Shuo, G.; Zhao, Y.Y.; Qu, H.C.; Wu, D.X.; Xu, H.; Li, C.; Liu, Y.; Zhu, X.Y.; Wang, Z.K. Geological characteristics and ore-forming time of the Dexing porphyry copper ore mine in Jiangxi Province. *Acta Geol. Sin.-Engl.* **2012**, *86*, 691–699. [CrossRef]
15. Zheng, Y.F.; Xiao, W.J.; Zhao, G.C. Introduction to tectonics of China. *Gondwana Res.* **2013**, *23*, 1189–1206. [CrossRef]
16. Zhou, X.M.; Sun, T.; Shen, W.Z.; Shu, L.S.; Niu, Y.L. Petrogenesis of Mesozoic granitoids and volcanic rocks in South China: A response to tectonic evolution. *Episodes* **2006**, *29*, 26–33. [CrossRef]
17. Maruyama, S. Pacific-type orogeny revisited: Miyashiro-type orogeny proposed. *Isl. Arc* **1997**, *6*, 91–120. [CrossRef]
18. Zhou, X.; Li, W. Origin of Late Mesozoic igneous rocks in Southeastern China: Implications for lithosphere subduction and underplating of mafic magmas. *Tectonophysics* **2000**, *326*, 269–287. [CrossRef]
19. Wang, Y.B.; Zeng, Q.D.; Liu, J.M.; Zhou, L.L. The late Early Cretaceous Mo mineralization in the South China Mo Province: Constraints from U–Pb and Re–Os geochronology of the Lufeng porphyry Mo deposit. *Acta Geol. Sin.-Engl.* **2019**, *93*, 1773–1782. [CrossRef]
20. Wang, Y.B.; Zeng, Q.D.; Liu, J.M.; Qin, K.Z.; Wu, L. Porphyry Mo and epithermal Au–Ag–Pb–Zn mineralization in the Zhilingtou polymetallic deposit, South China. *Miner. Depos.* **2020**, *55*, 1385–1406. [CrossRef]
21. Li, X.H.; Li, W.X.; Li, Z.X.; Lo, C.H.; Wang, J.; Ye, M.F.; Yang, Y.H. Amalgamation between the Yangtze and Cathaysia Blocks in South China: Constraints from SHRIMP U–Pb zircon ages, geochemistry and Nd–Hf isotopes of the Shuangxiwu volcanic rocks. *Precambrian Res.* **2009**, *174*, 117–128. [CrossRef]
22. Zhang, S.B.; Zheng, Y.F. Formation and evolution of Precambrian continental lithosphere in South China. *Gondwana Res.* **2013**, *23*, 1241–1260. [CrossRef]
23. Pirajno, F.; Bagas, L.; Hickman, A.H.; Gold Research Team. Gold mineralization of the Chencai-Suichang uplift and tectonic evolution of Zhejiang province, Southeast China. *Ore Geol. Rev.* **1997**, *12*, 35–55. [CrossRef]
24. Wang, Y.B.; Zeng, Q.D.; Zhang, S.; Chen, P.W.; Gao, S. Spatial–temporal relationships of late Mesozoic granitoids in Zhejiang Province, Southeast China: Constraints on tectonic evolution. *Int. Geol. Rev.* **2018**, *60*, 1529–1559. [CrossRef]
25. Li, Y.J.; Wei, J.H.; Chen, H.Y.; Tan, J.; Fu, L.B.; Wu, G. Origin of the Maoduan Pb-Zn-Mo deposit, eastern Cathaysia Block, China: Geological, geochronological, geohemical, and Sr–Nd–Pb–S isotopic constraints. *Miner. Depos.* **2012**, *47*, 763–780. [CrossRef]
26. Zhu, A.Q.; Zhang, Y.S.; Lu, Z.D.; Zhang, C.L. Metallogenic series and belts of the metal and nonmetallic deposits of Zhejiang Province. *Beijing Geol. Publ. House* **2009**, 1–433. (In Chinese)

27. Li, X.H.; Liu, Y.; Li, Q.L.; Guo, C.H. Precise determination of Phanerozoic zircon Pb/Pb age by multi-collector SIMS without external standardization. *Geochem. Geophys. Geosyst.* **2009**, *10*, Q04010. [CrossRef]

28. Du, A.D.; He, H.L.; Yin, N.W.; Zou, X.Q.; Sun, Y.L.; Sun, D.Z.; Chen, S.Z.; Qu, W.J. A study of the rhenium-osmium geochronometry of molybdenites. *Acta Geol. Sin.* **1994**, *68*, 339–347. (In Chinese with English Abstract).

29. Du, A.D.; Wu, S.Q.; Sun, D.Z.; Wang, S.X.; Qu, W.J.; Markey, R.; Stein, H.; Morgan, J.W.; Malinovskiy, D. Preparation and Certification of Re–Os Dating Reference Materials: Molybdenite HLP and JDC. *Geostandard. Geoanal. Res.* **2004**, *28*, 41–52. [CrossRef]

30. Wu, Y.B.; Zheng, Y.F. Genesis of zircon and its constraints on interpretation of U–Pb age. *Chin. Sci. Bull.* **2004**, *49*, 1554–1569. (In Chinese with English Abstract). [CrossRef]

31. Smoliar, M.I.; Walker, R.J.; Morgan, J.W. Re–Os ages of group IIA, IIIA, IVA and VIB iron meteorites. *Science* **1996**, *271*, 1099–1102. [CrossRef]

32. Tang, Z.C.; Dong, X.F.; Hu, W.J.; Meng, X.S.; Rong, Y.P. SHRIMP zircon U-Pb dating of Xianlin granodiorite rock in Western Zhejiang and their geological significance. *Geoscience* **2014**, *28*, 884–891. (In Chinese with English Abstract).

33. Wang, Y.B.; Zeng, Q.D.; Qu, W.J. Ore-forming age and geological significance of there-stage Mo polymetallic deposits in the Zhejiang province. *Acta Mineral. Sin.* **2013**, *33*, 55–56. (In Chinese)

34. Hu, K.M.; Tang, Z.C.; Meng, X.S.; Zhou, H.W.; Dong, X.F.; Du, X.; Chen, Z.D. Chronology of petrogenesis and mineralization of the Datongkeng porphyry W-Mo deposit in Western Zhejiang. *Earth Sci.* **2016**, *41*, 1435–1450. (In Chinese with English Abstract).

35. Tang, Y.W.; Xie, Y.L.; Liu, L.; Lan, T.G.; Yang, J.L.; Sebastien, M.; Yin, R.C.; Liang, S.S.; Zhou, L.M. U–Pb, Re–Os and Ar–Ar dating of the Linghou polymetallic deposit, Southeastern China: Implications for metallogenesis of the Qingzhou–Hangzhou metallogenic belt. *J. Asian Earth Sci.* **2017**, *137*, 163–179. [CrossRef]

36. Chen, T.L.; Ren, Z.; Li, K.X.; Liu, F.; Duan, F.H.; Leng, C.B. Distribution characteristics and influencing factors of rhenium concentrations in molybdenite from the porphyry Cu-systems: A review. *Acta Petrol. Sin.* **2021**, *37*, 2677–2690. (In Chinese with English Abstract).

37. Tang, Y.W.; Xie, Y.L.; Li, Y.X.; Qiu, L.M.; Zhang, X.X.; Han, Y.D.; Jiang, Y.C. LA–ICP–MS U–Pb Ages, geochemical characteristics of the zircons from Wushanguan complex body in Anji mining area, Northwestern Zhejiang and their geological significances. *Geol. Rev.* **2013**, *59*, 702–715. (In Chinese with English Abstract).

38. Wang, Y.B.; Feng, P.L.; Zhou, L.L.; Zeng, Q.D. Genetic links of porphyry Mo-epithermal Pb–Zn–Ag mineralization system: A case study of the Shipingchuan polymetallic deposit, South China. *Acta Geochim.* **2022**, *41*, 307–323. [CrossRef]

39. Kerrich, R.; Goldfarb, R.J.; Richards, J.P. Metallogenic provinces in an evolving geodynamic framework. *Econ. Geol.* **2005**, *100*, 1097–1136.

40. Chen, S.Q. Discussion on the Yanshan Epoch Rock Characteristics and Ore-Forming Background in Zhejiang Kaihua Region. Master's Thesis, China University of Geosciences, Beijing, China, 2011; pp. 21–30.

41. Jia, S.H.; Zhao, Y.Y.; Wang, Z.Q.; Wu, Y.D.; Wang, T.; Chen, L. Zircon U–Pb dating and geochemical characteristics of granodiorite-porphyry in the Linghou copper deposit, Western Zhejiang, and their geological significance. *Acta Geol. Sin.* **2014**, *88*, 2071–2085. (In Chinese with English Abstract).

42. Xiong, X.L.; Adam, J.; Green, T.H. Trace element characteristics of partial melts produced by melting of metabasalt at high pressures: Constraints on the formation condition of adakitic melts. *Sci. China Ser. D* **2006**, *49*, 915–925. [CrossRef]

43. Wu, F.Y.; Ji, W.Q.; Sun, D.H.; Yang, Y.H.; Li, X.H. Zircon U–Pb geochronology and Hf isotopic compositions of the Mesozoic granites in southern Anhui Province, China. *Lithos* **2012**, *150*, 6–25. [CrossRef]

44. Jiang, Y.H.; Jiang, S.Y.; Dai, B.Z.; Liao, S.Y.; Zhao, K.D.; Ling, H.F. Middle to late Jurassic felsic and mafic magmatism in southern Hunan province, southeast China: Implications for a continental arc to rifting. *Lithos* **2009**, *107*, 185–204. [CrossRef]

45. Defant, M.J.; Drummond, M.S. Derivation of some modern arc magmas by melting of young subduction lithosphere. *Nature* **1990**, *347*, 662–665. [CrossRef]

46. Yang, S.Y.; Jiang, S.Y.; Zhao, K.D.; Jiang, Y.H.; Ling, H.F.; Luo, L. Geochronology, geochemistry and tectonic significance of two Early Cretaceous A-type granites in the Gan-Hang Belt, Southeast China. *Lithos* **2012**, *150*, 155–170. [CrossRef]

47. Li, Z.L.; Zhou, J.; Mao, J.R.; Santosh, M.; Yu, M.G.; Li, Y.Q.; Hu, Y.Z.; Langmuir, C.H.; Chen, Z.X.; Cai, X.X.; et al. Zircon U–Pb geochronology and geochemistry of two episodes of granitoids from the northwestern Zhejiang province, SE China: Implication for magmatic evolution and tectonic transition. *Lithos* **2013**, *179*, 334–352. [CrossRef]

48. Li, Y.J.; Wei, J.H.; Yao, C.L.; Yan, Y.F.; Tan, J.; Fu, L.B.; Pan, J.B.; Li, W. Zircon U–Pb dating and tectonic significance of the Shipingchuan granite in Southeastern Zhejiang province, SE China. *Geol. Rev.* **2009**, *55*, 673–683. (In Chinese with English Abstract).

49. Liu, Q.; Yu, J.H.; Wang, Q.; Su, B.; Zhou, M.F.; Xu, H.; Cui, X. Ages and geochemistry of granites in the Pingtan–Dongshan Metamorphic Belt, Coastal South China: New constraints on late Mesozoic magmatic evolution. *Lithos* **2012**, *150*, 268–286. [CrossRef]

50. Li, J.H.; Zhang, Y.Q.; Dong, S.W.; Johnston, S.T. Cretaceous tectonic evolution of South China: A preliminary synthesis. *Earth Sci. Rev.* **2014**, *134*, 98–136. [CrossRef]

51. Rapp, R.P.; Shimizu, N.; Norman, M.D.; Applegate, G.S. Reaction between slab-derived melts and peridotite in the mantle wedge: Experimental constraints at 3.8 GPa. *Chem. Geol.* **1999**, *160*, 335–356. [CrossRef]

52. Jiang, Y.H.; Zhao, P.; Zhou, Q.; Liao, S.Y.; Jin, G.D. Petrogenesis and tectonic implications of Early Cretaceous S- and A-type granites in the northwest of the Gan-Hang rift, SE China. *Lithos* **2011**, *121*, 55–73. [CrossRef]